Identification, expression analysis, and potential roles of microRNAs in the regulation of polysaccharide biosynthesis in Polygonatum cyrtonema Hua

Kelong Ma
Anhui University of Chinese Medicine
Shengxiang Zhang
Anhui University of Chinese Medicine
Daiyin Peng
Anhui University of Chinese Medicine
Chenkai Wang
Anhui University of Chinese Medicine
Yuanyuan Shi
Anhui University of Chinese Medicine
Qingshan Yang
Anhui University of Chinese Medicine
jiawen Wu (wujiawen@ahtcm.edu.cn)
Anhui University of Traditional Chinese Medicine https://orcid.org/0000-0003-4407-6819
Luqi Huang
China Academy of Chinese Medical Sciences

Research article

Keywords: Polygonatum cyrtonema Hua, RNA-Seq, miRNAome, polysaccharides, metabolic pathways, gene expression

Posted Date: May 29th, 2019

DOI: https://doi.org/10.21203/rs.2.9936/v1

Version of Record: A version of this preprint was published at Journal of Plant Biochemistry and Biotechnology on February 18th, 2022. See the published version at https://doi.org/10.1007/s13562-022-00772-7.

Abstract

Background: MicroRNAs (miRNAs) are a group of endogenous small non-coding RNAs with important roles in plant growth, development, and metabolic processes. Polygonatum cyrtonema Hua (P. cyrtonema) is an important Chinese traditional medicinal herb with broad pharmacological functions, and polysaccharides are the main biological substance accumulated in the P. cyrtonema rhizome. However, regulation of the process of polysaccharide biosynthesis in P. cyrtonema remains largely unknown. Results: To elucidate the miRNAs and their targets involved in polysaccharide biosynthesis in P. cyrtonema, four small RNA libraries were constructed from flower, leaf, rhizome, and root tissues and sequenced. A total of 69 conserved and 5 novel miRNAs were identified, of which 6 miRNAs (miR156a-5p, miR156f-5p, miR395a_5, miR396a-3p, miR396g-3p, and miR397-5p_1) were down-regulated and 7 miRNAs (miR160, miR160h_1, miR160e-5p, miR319b_1, miR319_1, miR319c-5p_3, and miR319c_1) were up-regulated in rhizomes compared with flower, leaf, and root tissues. Bioinformatics analysis showed that the predicted targets of these miRNAs were mostly transcription factors and functional genes enriched in metabolic and secondary metabolite biosynthetic pathways, and 7 genes and their paired miRNAs were identified in carbohydrate metabolism. qRT-PCR expression analysis demonstrated that 6 miRNAs and their targets involved in carbohydrate metabolism were existed a negative correlation in. P. cyrtonema tissues. MiR396a-3p and one of its target genes, abfA, were possibly involed in polysaccharide biosynthesis pathway. Conclusions: This is the first report on the identification of conserved and novel miRNAs and their potential targets in P. cyrtonema, thus providing molecular evidence for the role of miRNAs in the regulation of polysaccharide biosynthesis in P. cyrtonema.

Background

Polygonatum cyrtonema Hua (Liliaceae) is a perennial plant that grows mainly in the temperate regions of the northern hemisphere, including China, Japan, Korea, and Russia [1]. Due to its antioxidant, anti-aging, and neuroprotective effects, *P. cyrtonema* is widely used as a traditional Chinese medicine for the treatment of cardiovascular and other diseases in China [2, 3]. The rich biological activity of *P. cyrtonema* is attributed to the presence of various compounds such as alkaloids, flavonoids, steroidal saponins, lignin, and polysaccharides[2, 4], and polysaccharides are considered as one of the most important groups of active compounds in *P. cyrtonema* [5, 6]. Recently, *P. cyrtonema* polysaccharides have gained more attention for their various pharmacological applications and biological activities. However, most of the research is focused on the extraction, chemical composition, and molecular structure of polysaccharides, and few studies are conducted on the genetic and epigenetic regulation of polysaccharides in *P. cyrtonema*. Consequently, molecular mechanisms of polysaccharide biosynthesis and regulation remain unknown.

MicroRNAs (miRNAs) are a group of small non-coding RNAs that play crucial roles in various biological and metabolic processes underlying plant growth and development [7]. Generally, miRNAs exhibit tissue or stage-specific expression patterns, and participate in the regulation of the accumulation of secondary metabolites such as steroids and ketones by negatively regulating the expression of target genes[8-10]. For instance, miRNAs are involved in the biosynthesis of terpenoid indole alkaloids in *Catharanthus roseus*[11]. Additionally, *miR156*, *miR828*, *miR858*, and *miR5072* regulate anthocyanin accumulation in apple peel[12]. In Brazilian rubber tree, *miR159b* regulates the production of latex[13]. Therefore, the identification of miRNAs and their

target genes is essential for understanding the regulation of miRNA-mediated biosynthesis of polysaccharides in *P. cyrtonema*.

Because miRNAs are important regulators of gene expression, they have been thoroughly studied in many species. However, despite the medicinal significance of *P. cyrtonema*, miRNAs have not yet been identified in this species. Therefore, the aim of this study was to identify conserved and novel miRNAs and their potential target genes in *P. cyrtonema.* To achieve this goal, we sequenced small RNAs (sRNAs) from different tissues of *P. cyrtonema* using the BGISEQ-500 platform, analyzed miRNA expression profiles, and investigated the functions of target genes. Quantitative real-time PCR (qRT-PCR) was used to verify the results of sRNA sequencing and to identify candidate genes involved in the accumulation of polysaccharides in *P. cyrtonema*. Our results provide valuable information on the miRNAs involved in polysaccharide biosynthesis in*P. cyrtonema.*

Results

De novo sRNA-seq analysis

To identify miRNAs in *P. cyrtonema*, four cDNA libraries prepared from flower, leaf, rhizome, and root tissues were sequenced using the BGI BGISEQ-500 sequencing technology. Approximately 162 million raw reads were generated from the cDNA libraries. The raw reads were cleaned to obtain 36,516,720 reads from flower library (PcH_F), 41,537,414 reads from leaf library (PcH_L), 35,905,873 reads from rhizome library (PcH_RH), and 32,754,124 reads from root library (PcH_R) (Figure 1a, Table S1). The quality score (Q20) of all four libraries exceeded 99%, indicating good quality sequence data. The distribution of base quality in clean reads is shown in Figure S1. Analysis of the length and composition of sRNAs revealed that 24-nt long sRNAs were the most abundant in the four libraries, followed by 21-nt and 22-nt sRNAs (Figure 1b). In the PcH_F, PcH_L, PcH_RH, and PcH_R libraries, 24-nt sRNAs accounted for 39.42%, 29.28%, 36.79%, and 18.47% of all sRNAs, respectively; similarly, 21-nt sRNAs accounted for 15.81%, 19.88%, 16.03%, and 12.29% of all sRNAs, respectively, while 22-nt sRNAs accounted for 9.21%, 11.77%, 13.42%, and 12.74% of all sRNAs, respectively. The remaining sRNAs accounted for less than 10% of each sample.

Identification of conserved and novel miRNAs

To identify miRNAs, all clean reads were mapped against the known sRNA databases including miRBase, Rfam, siRNA, and snoRNA. The mapping rates of PcH_F, PcH_L, PcH_RH, and PcH_R libraries were 15.04% (5,491,711 reads), 18.26% (7,586,026 reads), 15.87% (5,697,605 reads) and 25.73% (8,426,412 reads), respectively (Table S2). All sRNAs were classified into different categories, according to their annotations, and the proportion of sRNAs in each category is shown in Figure S2.

A total of 20 miRNA families comprising 69 conserved miRNAs were identified in *P. cyrtonema*; 65 in PcH_F, 59 in PcH_L, 62 in PcH_RH, and 57 in PcH_R (Figure 2a, Table S4). The length of conserved miRNAs varied from 18–22 nt, the majority of which were 21-nt long (37 out of 69 conserved miRNAs; 53.62%), followed by 20-nt miRNAs (23 out of 69 conserved miRNAs; 33.33%) (Table S3). Precursors of conserved miRNAs were also identified, with lengths ranging from 19–269 nt. Statistical analysis of the first base of predicted miRNAs

showed a strong preference for uridine (U) in 21-nt long miRNAs (Figure S3a and 3b). The largest family identified was *miR319* with 10 members, followed by *miR396* and *miR166*, with 8 and 7 members, respectively. Of the remaining 17 families, 12 families were represented by 2-13 members while 5 were represented by a single member (Figure 2b).

Interestingly, the abundance of miRNAs in each miRNA family varied considerably. The most abundant miRNA was *miR159a_1* (read counts in the PcH_L library > 470,000) as well as *miR168a-5p* and *miR166g-3p* (read counts exceeding 10,000 in each library), whereas *miR390.1*, *miR171c-5p_1*, *miR396g*, *miR390a-3p*, *miR319f_1*, *miR395b-3p*, *miR477b_1*, and *miR156b_2* showed the lowest abundance (read counts < 5) (Table S4). In addition, the miRNAs showed a very broad range of expression, ranging from millions of reads to less than 10 reads, as expected. Some miRNAs showed clear tissue-specific expression. For instance, the expression level of *miR319a_1*, *miR319a-3p*, *miR319b_1*, *miR319_1*, *miR319c_1*, *miR319c_2*, *miR8175*, and *miR160* was significantly higher in rhizomes than in other tissues. Similarly, the expression level of *miR396a-5p*, *miR166a-3p*, *miR168a-3p*, and *miR166h-3p_1* was significantly higher in flowers, that of *miR171b_2*, *miR167d-5p*, *miR159a_1*, *miR171b-3p*, *miR166a-3p*, and *miR167d_1* was higher in leaves, and that of *miR168a-5p* and *miR168* was higher in roots than in other tissues (Table S4).

To predict potentially novel miRNAs in *P. cyrtonema*, miRDeep2 and miRA software were used to explore the stem-loop hairpin secondary structures and enzyme cleavage sites, and the minimum free energy of novel miRNAs was measured. Five new hairpin miRNA candidates, ranging from 21–30 nt in length, were identified. These miRNA candidates were potentially new miRNAs or new members of conserved miRNA families in *P. cyrtonema*. (Table S5).The precursors of novel miRNAs ranged from 76–248 nt in length (average = 156 nt), which is consistent with the typical length distribution of mature miRNAs. Nucleotide bias analysis showed that new miRNAs had similar tendency of conserved miRNA in all libraries (Figure S4). The abundance of novel miRNAs in different tissues varied significantly. For instance, the number of *novel_miR4* in flower and leaf tissues was much higher than that in rhizome and root tissues. By contrast, the abundance of *novel_miR3* and *novel_miR5* was low; these were detected only in flower and leaf tissues, respectively. Similarly, *novel_miR2* was detected only in leaves, whereas *novel_miR1* was detected in all four tissues, except roots (Table S6).

Differential expression analysis of miRNAs

Based on the number of reads that mapped to the *P. cyrtonema* genome, the expression level of sRNAs was calculated as Transcripts Per kilobase Million (TPM). Correlation analysis showed that the overall expression pattern of sRNAs in rhizomes was similar to that in roots (Pearson's correlation coefficient = 1.0) but different from that in flowers and leaves (Figure S5).

Since polysaccharides mainly accumulate in rhizomes, we further investigated the miRNAs expressed in rhizomes. The number of up-regulated and down-regulated miRNAs in rhizomes were 20 and 49 compared with flowers, 34 and 37 compared with leaves, and 45 and 24 compared with roots, respectively (Figure 3a, Table S7). The total miRNA expression level in rhizome was the same as that in leaf, lower in flower, and higher than root. (Figure 3b). To further investigate miRNAs showing differential expression between the rhizome vs. three other tissues, we performed hierarchical cluster analysis of miRNAs using the heatmap function in R software (Figure 3c). Specifically, the expression level of *miR156a-5p*, *miR156f-5p*, *miR395a_5*, *miR396a-3p*,

miR396g-3p, and *miR397-5p_1* in rhizome was significantly lower than that in flower, leaf, and root, whereas the expression level of miR160, miR160h_1, miR160e-5p, miR319b_1, miR319_1, miR319c-5p_3, and *miR319c_1* in rhizome was significantly higher than that in flower, leaf, and root(Table S7).

Prediction of miRNA target genes

To better understand the potential functions of the miRNAs in *P. cyrtonema*, it is necessary to predict and confirm their target genes. A total of 1,525 target genes were predicted for 81 miRNAs, of which 1239 genes were predicted using psRobot, 824 using TargetFinder, and 934 were predicted repeatedly. After data filtering, 69 miRNAs had a total of 499 target genes (Table S8), and most of the predicted target genes were involved in a variety of biological processes, including transcriptional regulation, signal transduction, and stress response (Table S9).

It is known that one miRNA may have several target genes. In our study, the number of target genes varied significantly among miRNAs. For example, *miR172a_4* was predicted to have 45 target genes, while *miR160a-5p* and *novel_mir4* had only one target. In addition, some miRNAs from the same family or different families were predicted to regulate the same target gene (Table S9). For example, the squamosa promoter-binding protein-like (*SPL*) transcription factor encoding gene was predicted as the target of *miR156a-5p*, *miR156b_2*, *miR156f-5p*, *miR529e_1*, and *miR529h*, whereas genes encoding *MYB* transcription factors were predicted as targets of *miR159a_1*, *miR319_1*, *miR319a-3p*, *miR319b_1*, *miR319c_1*, *miR319c_2*, *miR319f_1*, *miR319g*, *miR319_1*, and *miR858b*. Auxin response factors (*ARFs*) play an important role in plant growth, development, and adaptive responses, and *ARF* genes were predicted as targets of *miR160a-5p*, *miR160b_1*, *miR160e-5p*, *miR160h_1*, and *miR167d_1*. (Table S9).

Although the expression level of novel miRNAs was lower than that of conserved miRNAs, novel miRNAs were found to have candidate target genes, including transcription factor encoding genes and functional genes. For example, gene encoding mannose-specific lectin precursor was predicted as the target of *novel_miR1*; genes encoding low-temperature-induced 65 kDa protein and ABC transporter C family member as targets of *novel_miR2*, and those encoding the hypothetical protein, peroxisomal adenine nucleotide carrier 1, and probable protein phosphatase 2C 38 as targets of *novel_miR4* (Table S9).

Annotation of miRNA target genes

To gain insights into the possible roles of DEMs, their putative target genes annotated using gene ontology (GO) enrichment analysis. GO analysis grouped the target genes into three main categories: biological process, cellular component, and molecular function. In the biological process category, target genes were associated with cellular process, single organism process, metabolic process, and biological regulation; the number of genes associated with each of these terms was 48, 39, 38, and 18 in the rhizome vs. flower group (Figure 4a), 37, 35, 31, and 17 in the rhizome vs. leaf group (Figure 4b), and 31, 16, 23, and 18 in the rhizome vs. root group (Figure 4c). Thus, the number of differentially expressed genes identified in the rhizome vs. root group was smaller than that identified in the rhizome vs. leaf and rhizome vs. flower groups.

In the cellular component category, target genes were mainly enriched in cell, cell part, and membrane. There was no significant difference in the number of genes enriched in different tissues. However, in the molecular function category, genes were enriched in binding, catalytic activity, and nucleic acid transcription factor activity; the number of genes associated with catalytic activity were 44 in the rhizome vs. flower group, 30 in the rhizome vs. leaf group, and 26 in the rhizome vs. root group.

Genes usually act in networks to regulate biological functions, and pathway-based analysis such as Kyoto Encyclopedia of Genes and Genomes (KEGG) enrichment analysis helps to understand the biological functions of these target genes. The results of KEGG enrichment analysis showed that target genes of DEMs were involved in 42 pathways in the rhizome vs. flower group (Figure 5a, Table S10), 39 pathways in the rhizome vs. leaf group (Figure 5b, Table S11), and 38 pathways in the rhizome vs. root group (Figure 5c, Table S12). In addition to plant hormone signal transduction, most of these pathways were involved in biomaterial metabolism, such as metabolism of sugars, amino acids, lipids, and nucleotides and biosynthesis of secondary metabolites.

Identification of miRNAs and their putative target genes related to polysaccharide biosynthesis

In plants, miRNAs have been associated with secondary metabolism, polysaccharide metabolism, and other biological processes. Here, we screened and analyzed target genes of DEMs and identified seven genes and their paired miRNAs involved in carbohydrate metabolism including those encoding alpha-L-arabinofuranosidase (*abfA*, *miR396a-3p* target), L-galactose dehydrogenase (*GalDH*, *miR8175* target), berberine bridge enzyme-like 18 (*miR396h* target), L-iditol 2-dehydrogenase (*SORD*, *miR396b* target), *MACPF* domain-containing protein *CAD1* (*miR168b* target), succinate dehydrogenase (*SDHA, miR397-5p* target) and an uncharacterized protein encoding gene LOC105157180 *(miR390a-5p* target) (Table 1). Among these miRNAs, *miR396a-3p*, *miR396b*, and *miR168b* were up-regulated in rhizomes compared with other tissues, whereas *miR390a-5p* and *miR396h* were down-regulated in the rhizome. Additionally, the expression level of *miR8175* was the highest in the root and that of *miR397-5p* which was the lowest in all tissues (Figure 6a). The abundance of *abfA*, *GalDH*, *SORD*, and *SDHA* transcripts was inversely correlated with that of their miRNAs (Figure 6b), suggesting the possibility of a regulated mechanism. These genes may participate in polysaccharide biosynthesis in *P. cyrtonema*.

Validation of miRNA expression by qRT-PCR

To verify sRNA-Seq data, expression levels of four miRNAs (miR396a-3p, miR396g-3p, miR156a-5p, miR828a,) and their predicted target genes were verified by qRT-PCR using primers listed in Table S13. The expression levels of these four miRNAs were consistent with those of sRNA-Seq analysis, and exhibited a negative correlation with those of their putative target genes (Figure 7). For example, compared with flowers and leaves, the expression of miR396a-3p, miR156a-5p and miR828a was significantly down-regulated in rhizomes and roots, whereas that of their target genes were up-regulated. miR396g-3p was up-regulated in leaves and rhizomes, whereas its target gene was down-regulated in these two tissues.

Polysaccharides are a group of secondary metabolites whose biosynthesis may be controlled by target genes identified in this study. The putative target gene of miR396a-3p was predicted encode abfA, an enzyme in the amino sugar and nucleotide sugar metabolism pathway, which is associated with the biosynthesis of *L-arabinan*. We constructed a three-dimensional (3D) structural model of *abfA* (CL6296.contig-1), based on the crystal structure of GH-51 arabinofuranosidase form *Thermobacillus xylanilyticus* (Tx-Abf) (PDB ID: 2vrk) using the SWISS-MODEL (https://swissmodel.expasy.org/) and PyMOL software[14]. The overall structure of *abfA* showed two characteristic GH-51 domains, namely, the N-terminal catalytic domain folded into a (β7/α8)-barrel in Tx-Abf (Figure 8a) and a C-terminal domain with jelly-roll topology (Figure 8b). Alignment of the three *abfA* amino acid sequences revealed that they all possess a well-conserved binding site (W297) and two active sites (E385 and E462) (Figure 8c and 8d).

Discussion

Polygonatum polysaccharides (PSPs) is an important biologically active substance of *P. sibiricum* Red, *P. cyrtonema* Hua, and *P. kingianum Coll*. et Hemsl. Previous studies have mainly focused on the transcriptome and pharmacological effects of this genus[15]. In this study, we identified miRNAs and their target genes involved in the biosynthesis of PSPs. Our results provide valuable information on the molecular mechanisms underlying PSP biosynthesis. Four sRNA libraries from flower, leaf, rhizome, and root tissues were constructed and sequenced, generating more than 32 million clean reads. The 24-nt sRNAs exhibited the highest abundance, which was consistent with the distribution pattern of sRNAs reported in *Panax notoginseng*[8]and *Medicago sativa* [16]. A total of 69 conserved miRNAs and 5 novel miRNAs were identified. Most of the miRNAs were highly conserved in plants, suggesting important regulatory roles of these miRNAs in plant growth and development.

Analysis of the spatiotemporal expression patterns of miRNAs provides useful information on the molecular function of these miRNAs. Analysis of conserved miRNAs revealed that *miR159a_1*, *miR168a-5p*, and *miR166g-3p* were highly expressed in all tissues. Among these miRNAs, miR159a_1 showed the highest expression level in leaves, which was consistent with expression pattern of *Eucommia ulmoides* [17]. In rhizomes, expression levels of *miR160*, *miR160e-5p*, *miR8175, miR319c_2*, *miR319b_1*, *miR319a_1*, *miR319a-3p*, and *miR319_1* were up-regulated and those of *miR167d-5p*, *miR171b_2*, *miR397a_3*, and *miR160a-5p* were significantly down-regulated compared with leaves and flowers. A previous study has shown that *miR160a* promotes leaf blade outgrowth as well as leaf and leaflet initiation and floral organ development through the quantitative regulation of its major target gene, *SlARF10A*[18]. Additionally, *miR160* plays a crucial role in local defense response and systemic acquired resistance (SAR) during the interaction between potato and *Phytophthora infestans*[19]. The *miR319a* indirectly regulates the development of pistils by regulating its target gene, *Pm-TCP4* [20]. Additionally, *miR319* and *TCP* gene families underlie robust and multilayer control of leaf development [21]. Similarly, *miR396a-5p* is an important conserved miRNA in plants; overexpression of *miR396a-5p* in tobacco increases tolerance to salt, drought, and cold stresses and susceptibility to *Phytophthora nicotianae* infection[22]. In this study, novel miRNAs showed lower abundance than conserved miRNAs, suggesting that these novel species-specific miRNAs are either young miRNAs that arose recently through evolution or more volatile than other miRNAs.

The miRNAs exhibit various biological roles by regulating the expression of their target genes. The predicted target genes of DEMs identified in this study showed a wide range of functions, including transcription factor genes and functional gene families related to plant growth and development and metabolite biosynthesis. For instance, gene encoding the *SPL* transcription factor, a major plant-specific transcription factor family [23, 24], was predicted as a target gene of *miR156a-5p*. A gene encoding *MYB* transcription factor was predicted as regulated by *miR159a_1*, *miR858b*, and *miR319* families, which participate in flavonol biosynthesisand drought or salt stress tolerance [25, 26] The *ARF* genes are a target of *miR160* and *miR167d*, which regulate plant growth and abiotic stress response [27, 28]. The target gene prediction of novel miRNAs revealed that the mannose-specific lectin precursor is regulated by *novel_miR1*. Genes encoding the low temperature-induced 65 kDa protein and ABC transporter C family member 5 was predicted as targets of *novel_miR2*, and those encoding peroxisomal adenine nucleotide carrier 1 and probable protein phosphatase 2C 38 were identified as targets of *novel_miR4*.

To identify miRNAs and their putative target genes related to polysaccharide biosynthesis, the target genes of DEMs involved in carbohydrate metabolism pathway were screened. Genes encoding *abfA*, *GalDH*, berberine bridge enzyme-like 18, *SORD*, *MACPF* domain-containing protein *CAD1*, an uncharacterized protein LOC105157180, and *SDHA* were predicted as targets of *miR396a-3p*, *miR8175*, *miR396h*, *miR396b*, *miR168b*, *miR390a-5p*, and *miR397-5p*, respectively. Moreover, PSPs mainly accumulate in the rhizome in *P. cyrtonema*, and *miR396a-3p*, *miR396b*, and *miR168b* were up-regulated in the rhizome compared with flower, leaf, and root. However, *miR390a-5p* and *miR396h* were down-regulated in the rhizome. Both *abfA* and *SORD* are key enzymes involved in carbohydrate metabolism, and these enzymes probably participate in polysaccharide biosynthesis in the rhizome of *P. cyrtonema*

Expression levels of four tissue-specific miRNAs (miR156a-5p, miR-828a, miR396a-3p, miR396g-3p) and their putative targets were validated by qRT-PCR assays. The expression patterns of four miRNAs were consistent with sRNA-Seq data and were inversely correlated with the expression pattern of their target genes. Previous studies have shown that *miR156a-5p* is involved in the regulation of the regulatory network involved in the response to viral infection in watermelon and other cucurbits [29]and stamen development in *Viburnum macrocephalum* f. *keteleeri* [30]. Additionally, *miR-828* is one of the conserved miRNAs in plants, which targets homoeologous *MYB2* genes that regulate trichome development in Arabidopsis and fiber development in cotton[31]and show strong associations with the color of tuber skin and tomato flesh [32]. Moreover, *miR396g* regulates genes associated with glucosylation and insolubilization of tannin precursors and the regulation of (de)astringency in persimmon fruits under normal development conditions [33]. Another miRNA, *miR396a*, regulates growth-regulating factor1 (*GRF1*), salicylic acid carboxyl methyltransferase (*SAMT*), glycosyl hydrolases (*GHs*), and nucleotide-binding site-leucine-rich repeat (*NBS-LRR*). Additionally, *miR396a-3p* is critical for abiotic stress tolerance in tomato by affecting salicylic acid (SA) or jasmonate (JA) signaling pathway by the negative regulation of target genes and their downstream genes[34]. Here, we found that *miR396a-3p* was down-regulated in roots and rhizomes of *P. cyrtonema* compared with leaves and flowers, while one of its target genes encoding *abfA* was up-regulated in rhizomes compared with other tissues. The *abfA* protein is an enzyme in the pentose and glucuronate interconversion pathway, suggesting its association with the biosynthesis of polysaccharides. Like Tx-Abf, *abfA* should be a retaining enzyme that catalyzes the hydrolysis of glycosidic bonds with Glu385 as the acid/base and Glu462 as the nucleophilea . Additionally, *abfA* (retaining enzyme) should be able to catalyze a wide variety of transglycosylation reactions.

Conclusions

This study is the first genome-wide investigation of miRNAs and their target genes in *P. cyrtonema*. Four sRNA libraries were generated from flower, leaf, rhizome and root tissues of *P. cyrtonema* and sequenced using a high-throughput sequencing technology. A total of 69 conserved and 5 novel miRNAs were identified, and their expression patterns, target genes, and functions were characterized. In addition, seven miRNAs and their target genes involved in the accumulation of PSPs were identified.

Although the foundation of the complex miRNA-mediated regulatory networks remains unresolved, this miRNA data set will help elucidate the gene regulatory networks in *P. cyrtonema* and other species. Therefore, our results act as a valuable resource for studying complex gene regulatory functions of miRNAs, especially during the process of polysaccharide biosynthesis in *P. cyrtonema*.

Methods

Sample collection

P. cyrtonema plants were collected from the Chinese Medicine herb garden of Anhui University of Chinese Medicine with permission of managers and Professionals, and authenticated by Prof. Qingshan Yang. Flowers, leaves, rhizomes and roots were collected from three randomly selected plants, pooled together and labeled as PcH_F, PcH_L, PcH_RH, and PcH_R, respectively. Tissues were cleaned with ultrapure water, dried on filter paper, and immediately frozen in liquid nitrogen for further analyses.

RNA isolation, sRNA library construction, and sequencing

Total RNA was isolated from flowers, leaves, rhizomes, and roots using RNA Plant Kit (Aidlab Biotech, Beijing, China), according to the manufacturer's instructions. RNA quality was evaluated using Agilent 2100 Bioanalyzer (Agilent Technologies, Palo Alto, CA, USA). Purified RNA was used to construct sRNA libraries, which were sequenced using the BGISEQ-500 platform at BGI Company, Wuhan, China.

Bioinformatics analysis and miRNA prediction

The raw sRNA-Seq reads were screened to remove the low quality reads including very short sequences, and sequences without the insert or with too long insert, low mass, or polyA. After filtering, the length distribution of clean reads was calculated and summarized. The clean reads were then mapped on to the reference genome and other sRNA databases using Bowtie2 (version 2.2.5)[35]. To ensure that each unique small RNA is mapped to only one category, we followed this priority rule: MiRbase > pirnabank > snoRNA (human/plant) > Rfam > other sRNA. miRDeep2 [36]and miRA[37]were used for novel miRNA prediction.

Analysis of DEMs

The expression level of sRNAs was calculated using Transcripts Per Kilobase Million (TPM)[38], which eliminates the influence of sequencing discrepancy on the calculation of sRNA expression. Therefore, the

calculated gene expression data could be directly used to compare the difference in gene expression between samples. T P M = C × 10 6 N where C represents the number of miRNA reads in the sample, and N represents the total number of mapped reads. The differential expression multiple of the gene between different samples was calculated based on the gene expression level (FPKM value). In our study, genes with FC ≥ 2.00 and false discovery rate (FDR) ≤ 0.001 by the Poisson Dis method were considered differentially expressed[39-41]. Based on the differential miRNA expression results, the pheatmap package of the R software was used for hierarchical clustering analysis.

Target gene prediction, GO function annotation, and KEGG pathway analysis

The target genes of miRNAs were predicted using psRobot[42]and TargetFinder[43].GO enrichment analysis finds all GO terms significantly enriched in a list of differential expression microRNAs (DEMs) target genes that correspond to specific biological functions. All genes were mapped to GO terms in the GO database (http://www.geneontology.org/), which calculates the number of genes associated with each term. The hypergeometric test was used to find significantly enriched GO terms in the input gene list. This test was based on GO-Term-Finder (http://www.yeastgenome.org/help/analyze/go-term-finder). The *P*-value was corrected using the Bonferroni method, and a corrected *P*-value ≤ 0.05 was considered as a threshold. GO terms fulfilling this condition were defined as significantly enriched. Pathway-based analysis helps to further understand the biological function of DEMs target genes. KEGG was used to perform pathway enrichment analysis using the same formula for calculations as in GO analysis.

Validation of sRNA-Seq data using qRT-PCR

To identify candidate genes involved in the regulation of polysaccharide biosynthesis, the expression level of four miRNAs and their potential target genes were selected for qRT-PCR. Total RNA was extracted from roots, rhizomes, leaves, and flowers using the TRIzol Reagent (Invitrogen, Carlsbad, CA, USA), according to the manufacturer's instructions. Primers for qRT-PCR were designed using Primer 5.0 (Premier Biosoft International, Palo Alto, CA, USA) (Table S12). The qRT-PCR was conducted on a PIKOREAL 96 Real-Time PCR System using QuantiNova SYBR Green PCR Kit (Qiagen,USA). The *-actin* gene was used as an internal reference for data normalization. Each PCR was performed in a reaction volume of 20 μl containing 10 μl of 2X SYBR Green mixture, 2 μl diluted cDNA, 0.5 μl forward primer, 0.5 μl reverse primer, and 7 μl double distilled water. The reaction conditions were as follows: 95°C for 2 min, followed by 40 cycles of 95°C for 5 s and 60°C for 10 s. Each sample was replicated at least three times. The relative expression level of each gene was calculated using the $2^{-\Delta\Delta Ct}$ method. All data were subjected to analysis of variance (ANOVA), and the results were presented as mean ± SD. Differences with $P < 0.05$ were considered to be statistically significant.

Abbreviations

miRNA : microRNA ; TF: transcriptome factor; qRT-PCR: quantitative real-time PCR; DEM: differentially expressed miRNA; GO: Gene ontology; KEGG: Kyoto Encyclopedia of Genes and Genomes; sRNA: small RNA; TPM: Transcripts er kilobase million; SPL: squamosa promoter-binding protein-like; ARF: auxin response factor;

MYB: v-myb avian myeloblastosis viral oncogene homolog; TCP: Teosinte branched1/Cincinnata/proliferating cell factor; abfA: alpha-L-arabinofuranosidase; GalDH: L-galactose dehydrogenase; SORD: L-iditol 2-dehydrogenase; SDHA: succinate dehydrogenase; PSPs: Polygonatum polysaccharides; GRF1: growth-regulating factor1; SAMT: salicylic acid carboxyl methyltransferase; GHs: glycosyl hydrolases; NBS-LRR: nucleotide-binding site-leucine-rich repeat.

Declarations

Ethics approval and consent to participate

Not applicable.

Consent for publication

Not applicable.

Availability of data and material

The sRNA-Seq data sets of four *P. cyrtonema* tissues have been deposited in NCBI Sequence Read Archive (SRA) database under the accession number PRJNA531804.

https://dataview.ncbi.nlm.nih.gov/object/PRJNA531804?reviewer=b5ccv4n8g98n0fpt340u5jsac4

The RNA-seq data sets of four P. cyrtonema tissues have been deposited in NCBI Sequence Read Archive (SRA) database under the accession number PRJNA532834.

https://dataview.ncbi.nlm.nih.gov/object/PRJNA532834?reviewer=19plj7brjopm0i0t99i4c86r1k

Competing interests

The authors declare no competing interests.

Funding

Financial support for the development and completion of this project was provided by startup funds through Sustainable Utilization of Famous Traditional Chinese Medicine Resources (Grant no. 2060302) and National Natural Science Foundation of China (Grant No. 81373598), Natural Science Foundation of Anhui Province of China (Grant No. 1608085MH177) and National students' platform for Innovation and Entrepreneurship Training Program (Grant No. 201810369050) providing experimental support. Publication costs were funded by Natural Science Research Grant of Higher Education of Anhui Province (Grant No. KJ2018ZD028).

Authors' contributions

Project design and guidance: J.W.W., D.Y.P., and L.Q.H. Experiments and data analysis: K.L.M., S.X.Z., C.K.W., and Y.Y.S. Manuscript preparation: K.L.M. Preparation of plant materials: Q.S.Y. All authors read and approved the final manuscript.

Acknowledgements

We thank the Beijing Genomics Institute for assistance with experiments, and Qingshan Yang for identifying plant materials.

References

1. Zhao P, Zhao C, Li X, Gao Q, Huang L, Xiao P, Gao W: The genus Polygonatum: A review of ethnopharmacology, phytochemistry and pharmacology. *Journal of ethnopharmacology* 2018, 214:274-291.

2. Zhao X, Li J: Chemical constituents of the genus Polygonatum and their role in medicinal treatment. *Natural product communications* 2015, 10(4):683-688.

3. Cui X, Wang S, Cao H, Guo H, Li Y, Xu F, Zheng M, Xi X, Han C: A Review: The Bioactivities and Pharmacological Applications of Polygonatum sibiricum polysaccharides. *Molecules* 2018, 23(5).

4. Yelithao K, Surayot U, Lee JH, You S: RAW264.7 Cell Activating Glucomannans Extracted from Rhizome of Polygonatum sibiricum. *Preventive nutrition and food science* 2016, 21(3):245-254.

5. Zhu X, Li Q, Lu F, Wang H, Yan S, Wang Q, Zhu W: Antiatherosclerotic Potential of Rhizoma Polygonati Polysaccharide in Hyperlipidemia-induced Atherosclerotic Hamsters. *Drug research* 2015, 65(9):479-483.

6. Zhang H, Cao Y, Chen L, Wang J, Tian Q, Wang N, Liu Z, Li J, Wang N, Wang X *et al*: A polysaccharide from Polygonatum sibiricum attenuates amyloid-beta-induced neurotoxicity in PC12 cells. *Carbohydrate polymers* 2015, 117:879-886.

7. Hou J, Lu D, Mason AS, Li B, Xiao M, An S, Fu D: Non-coding RNAs and transposable elements in plant genomes: emergence, regulatory mechanisms and roles in plant development and stress responses. *Planta* 2019.

8. Wei R, Qiu D, Wilson IW, Zhao H, Lu S, Miao J, Feng S, Bai L, Wu Q, Tu D *et al*: Identification of novel and conserved microRNAs in Panax notoginseng roots by high-throughput sequencing. *BMC genomics* 2015, 16:835.

9. Lee CH, Carroll BJ: Evolution and Diversification of Small RNA Pathways in Flowering Plants. *Plant & cell physiology* 2018, 59(11):2169-2187.

10. Megha S, Basu U, Joshi RK, Kav NNV: Physiological studies and genome-wide microRNA profiling of cold-stressed Brassica napus. *Plant physiology and biochemistry : PPB* 2018, 132:1-17.

11. Shen EM, Singh SK, Ghosh JS, Patra B, Paul P, Yuan L, Pattanaik S: The miRNAome of Catharanthus roseus: identification, expression analysis, and potential roles of microRNAs in regulation of terpenoid indole alkaloid biosynthesis. *Scientific reports* 2017, 7:43027.

12. Qu D, Yan F, Meng R, Jiang X, Yang H, Gao Z, Dong Y, Yang Y, Zhao Z: Identification of MicroRNAs and Their Targets Associated with Fruit-Bagging and Subsequent Sunlight Re-exposure in the "Granny Smith" Apple Exocarp Using High-Throughput Sequencing. *Frontiers in plant science* 2016, 7:27.

13. Gebelin V, Leclercq J, Kuswanhadi, Argout X, Chaidamsari T, Hu S, Tang C, Sarah G, Yang M, Montoro P: The small RNA profile in latex from Hevea brasiliensis trees is affected by tapping panel dryness. *Tree physiology* 2013, 33(10):1084-1098.

14. <The structure of the complex between Source Biochemistry SO 2008 Jul 15 47 28 7441 51[PMIDT18563919].PDF>.

15. Wang S, Wang B, Hua W, Niu J, Dang K, Qiang Y, Wang Z: De Novo Assembly and Analysis of Polygonatum sibiricum Transcriptome and Identification of Genes Involved in Polysaccharide Biosynthesis. *International journal of molecular sciences* 2017, 18(9).

16. Fan W, Zhang S, Du H, Sun X, Shi Y, Wang C: Genome-wide identification of different dormant Medicago sativa L. MicroRNAs in response to fall dormancy. *PloS one* 2014, 9(12):e114612.

17. Wang L, Du H, Wuyun TN: Genome-Wide Identification of MicroRNAs and Their Targets in the Leaves and Fruits of Eucommia ulmoides Using High-Throughput Sequencing. *Frontiers in plant science* 2016, 7:1632.

18. Damodharan S, Corem S, Gupta SK, Arazi T: Tuning of SlARF10A dosage by sly-miR160a is critical for auxin-mediated compound leaf and flower development. *The Plant journal : for cell and molecular biology* 2018, 96(4):855-868.

19. Natarajan B, Kalsi HS, Godbole P, Malankar N, Thiagarayaselvam A, Siddappa S, Thulasiram HV, Chakrabarti SK, Banerjee AK: MiRNA160 is associated with local defense and systemic acquired resistance against Phytophthora infestans infection in potato. *Journal of experimental botany* 2018, 69(8):2023-2036.

20. Wang W, Shi T, Ni X, Xu Y, Qu S, Gao Z: The role of miR319a and its target gene TCP4 in the regulation of pistil development in Prunus mume. *Genome* 2018, 61(1):43-48.

21. Koyama T, Sato F, Ohme-Takagi M: Roles of miR319 and TCP Transcription Factors in Leaf Development. *Plant physiology* 2017, 175(2):874-885.

22. Chen L, Luan Y, Zhai J: Sp-miR396a-5p acts as a stress-responsive genes regulator by conferring tolerance to abiotic stresses and susceptibility to Phytophthora nicotianae infection in transgenic tobacco. *Plant cell reports* 2015, 34(12):2013-2025.

23. Zeng RF, Zhou JJ, Liu SR, Gan ZM, Zhang JZ, Hu CG: Genome-Wide Identification and Characterization of SQUAMOSA-Promoter-Binding Protein (SBP) Genes Involved in the Flowering Development of Citrus Clementina. *Biomolecules* 2019, 9(2).

24. Li XY, Lin EP, Huang HH, Niu MY, Tong ZK, Zhang JH: Molecular Characterization of SQUAMOSA PROMOTER BINDING PROTEIN-LIKE (SPL) Gene Family in Betula luminifera. *Frontiers in plant science* 2018, 9:608.

25. Zhai R, Zhao Y, Wu M, Yang J, Li X, Liu H, Wu T, Liang F, Yang C, Wang Z *et al*: The MYB transcription factor PbMYB12b positively regulates flavonol biosynthesis in pear fruit. *BMC plant biology* 2019, 19(1):85.

26. Wu J, Jiang Y, Liang Y, Chen L, Chen W, Cheng B: Expression of the maize MYB transcription factor ZmMYB3R enhances drought and salt stress tolerance in transgenic plants. *Plant physiology and biochemistry : PPB* 2019, 137:179-188.

27. Liu N, Dong L, Deng X, Liu D, Liu Y, Li M, Hu Y, Yan Y: Genome-wide identification, molecular evolution, and expression analysis of auxin response factor (ARF) gene family in Brachypodium distachyon L. *BMC plant biology* 2018, 18(1):336.

28. Song S, Hao L, Zhao P, Xu Y, Zhong N, Zhang H, Liu N: Genome-wide Identification, Expression Profiling and Evolutionary Analysis of Auxin Response Factor Gene Family in Potato (Solanum tuberosum Group Phureja). *Scientific reports* 2019, 9(1):1755.

29. Sun Y, Niu X, Fan M: Genome-wide identification of cucumber green mottle mosaic virus-responsive microRNAs in watermelon. *Archives of virology* 2017, 162(9):2591-2602.

30. Li W, He Z, Zhang L, Lu Z, Xu J, Cui J, Wang L, Jin B: miRNAs involved in the development and differentiation of fertile and sterile flowers in Viburnum macrocephalum f. keteleeri. *BMC genomics* 2017, 18(1):783.

31. Guan X, Pang M, Nah G, Shi X, Ye W, Stelly DM, Chen ZJ: miR828 and miR858 regulate homoeologous MYB2 gene functions in Arabidopsis trichome and cotton fibre development. *Nature communications* 2014, 5:3050.

32. Bonar N, Liney M, Zhang R, Austin C, Dessoly J, Davidson D, Stephens J, McDougall G, Taylor M, Bryan GJ *et al*: Potato miR828 Is Associated With Purple Tuber Skin and Flesh Color. *Frontiers in plant science* 2018, 9:1742.

33. Luo Y, Zhang X, Luo Z, Zhang Q, Liu J: Identification and characterization of microRNAs from Chinese pollination constant non-astringent persimmon using high-throughput sequencing. *BMC plant biology* 2015, 15:11.

34. Chen L, Meng J, Zhai J, Xu P, Luan Y: MicroRNA396a-5p and -3p induce tomato disease susceptibility by suppressing target genes and upregulating salicylic acid. *Plant science : an international journal of experimental plant biology* 2017, 265:177-187.

35. Langmead B, Trapnell C, Pop M, Salzberg SL: Ultrafast and memory-efficient alignment of short DNA sequences to the human genome. *Genome biology* 2009, 10(3):R25.

36. Friedlander MR, Chen W, Adamidi C, Maaskola J, Einspanier R, Knespel S, Rajewsky N: Discovering microRNAs from deep sequencing data using miRDeep. *Nature biotechnology* 2008, 26(4):407-415.

37. Evers M, Huttner M, Dueck A, Meister G, Engelmann JC: miRA: adaptable novel miRNA identification in plants using small RNA sequencing data. *BMC bioinformatics* 2015, 16:370.

38. t Hoen PA, Ariyurek Y, Thygesen HH, Vreugdenhil E, Vossen RH, de Menezes RX, Boer JM, van Ommen GJ, den Dunnen JT: Deep sequencing-based expression analysis shows major advances in robustness, resolution and inter-lab portability over five microarray platforms. *Nucleic acids research* 2008, 36(21):e141.

39. Li W, Xu R, Yan X, Liang D, Zhang L, Qin X, Caiyin Q, Zhao G, Xiao W, Hu Z *et al*: De novo leaf and root transcriptome analysis to explore biosynthetic pathway of Celangulin V in Celastrus angulatus maxim. *BMC genomics* 2019, 20(1):7.

40. Zhao L, Zhang X, Qiu Z, Huang Y: De Novo Assembly and Characterization of the Xenocatantops brachycerus Transcriptome. *International journal of molecular sciences* 2018, 19(2).

41. Audic S, Claverie JM: The significance of digital gene expression profiles. *Genome research* 1997, 7(10):986-995.

42. Wu HJ, Ma YK, Chen T, Wang M, Wang XJ: PsRobot: a web-based plant small RNA meta-analysis toolbox. *Nucleic acids research* 2012, 40(Web Server issue):W22-28.

43. Fahlgren N, Carrington JC: miRNA Target Prediction in Plants. *Methods in molecular biology* 2010, 592:51-57.

Tables

Table 1. List of miRNAs and carbohydrate metabolic pathway target genes showing different expression between the rhizome and three other tissues of *P. cyrtonema*.

miRNA ID	Carbohydrate metabolism pathway	Pathway ID	Differential expression target gene		
			Rhizome VS. Flower	Rhizome VS.Leaf	Rhizome VS.Root
miR396a-3p	Amino sugar and nucleotide sugar metabolism	ko00520	abfA	abfA	
miR8175	Ascorbate and aldarate metabolism	ko00053	GalDH	GalDH	GalDH
miR396b	Fructose and mannose metabolism	ko00051			SORD
miR396b	Pentose and glucuronate interconversions	ko00040			SORD
miR397-5p	Citrate cycle (TCA cycle)	ko00020	SDHA		
miR168b	Amino sugar and nucleotide sugar metabolism	ko00520			CL1624.Contig3_All
miR168b	Starch and sucrose metabolism	ko00500			CL15613.Contig3_All
miR390a-5p	Pentose and glucuronate interconversions	ko00040	CL53.Contig3_All	CL53.Contig3_All	CL53.Contig3_All
miR396h	Galactose metabolism	ko00052	Unigene1620_All		
miR396h	Starch and sucrose metabolism	ko00500	Unigene1620_All		

Additional Files Legends

Figure S1. Distribution of base quality in clean reads in the four samples of *P. cyrtonema*. The X-axis indicates the base position in a read, and Y-axis indicates the base quality score.

Figure S2. Proportions of different types of sRNAs in *P. cyrtonema*.

Figure S3. The nucleotide bias of conserved miRNA. (a) The first nucleotide bias of sRNA. (b) The nucleotide bias of miRNA

Figure S4. The nucleotide bias of novel miRNA. (a) The first nucleotide bias of sRNA. (b) The nucleotide bias of miRNA

Figure S5. Correlation analysis of four samples of *P. cyrtonema*. Both X- and Y-axes indicate the sample name. Color indicates the Pearson's correlation coefficient (blue, high correlation; white, low correlation).

Table S1. Summary of sRNA-Seq data of each sample.

Table S2 Alignment statistics of tags align to reference genome.

Table S3. Details of conserved miRNAs identified in *P. cyrtonema*.

Table S4. Read counts of conserved miRNAs identified in *P. cyrtonema*.

Table S5. Details of novel miRNAs identified in *P. cyrtonema*.

Table S6. Read counts of novel miRNAs identified in *P. cyrtonema*.

Table S7. Differential expression of miRNAs in RH vs.F, RH vs.L and RH vs.R of P. cyrtonema.

Table S8. Statistics of miRNA target gene prediction in *P. cyrtonema*

Table S9. List of target genes predicted in *P. cyrtonema*.

Table S10. Statistics of pathway enrichment in rhizome vs. flower of *P. cyrtonema*.

Table S11. Statistics of pathway enrichment in rhizome vs. leaf of *P. cyrtonema*.

Table S12. Statistics of pathway enrichment in rhizome vs. root of *P. cyrtonema*.

Table S13. List of qRT-PCR primers used in this study.

Figures

Figure 1

Summary of sRNA-Seq data. (a) Characteristics of sRNA-Seq data obtained from each sample. (b) Length and abundance of unique sRNAs in the four libraries of P. cyrtonema.

Figure 2

Distribution of miRNAs identified in P. cyrtonema. (a) Number of miRNAs identified in flower, leaf, rhizome, and root tissues. (b) Number of miRNAs identified per family.

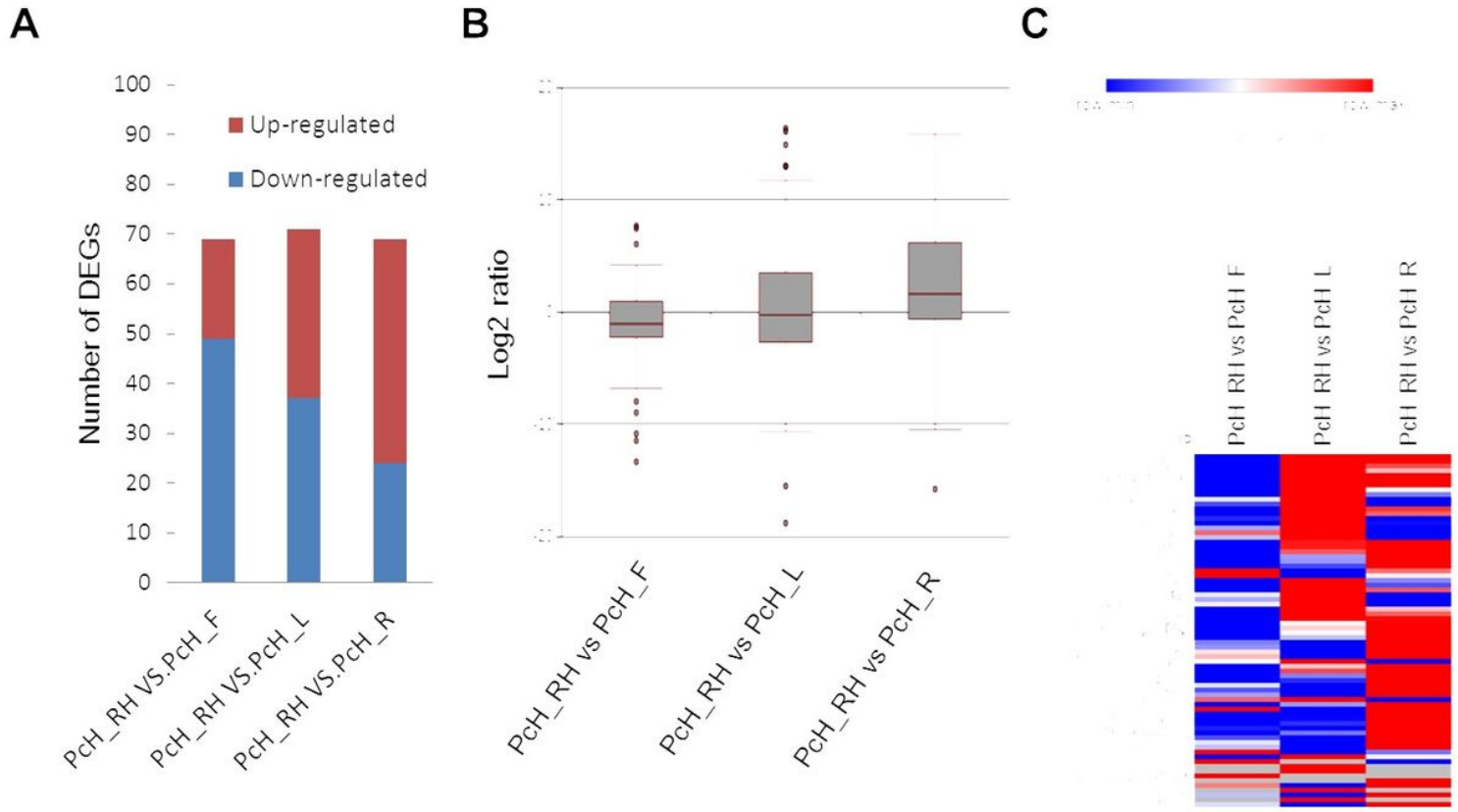

Figure 3

Expression patterns of miRNAs in P. cyrtonema. (a) Expression patterns of miRNAs in four groups. Up-regulated miRNAs are indicated in red, and down-regulated miRNAs are indicated in blue. (b) Boxplot of difffential expression of miRNAs (DEMs) in the rhizome compared with the other three tissues. X-axis represents the tissues, and Y-axis shows the log2 ratio values. (c) Hierarchical clustering analysis of DEMs in rhizomes compared with the other three tissues. The X-axis represents pairwise comparisons between samples, and Y-axis represents DEMs.

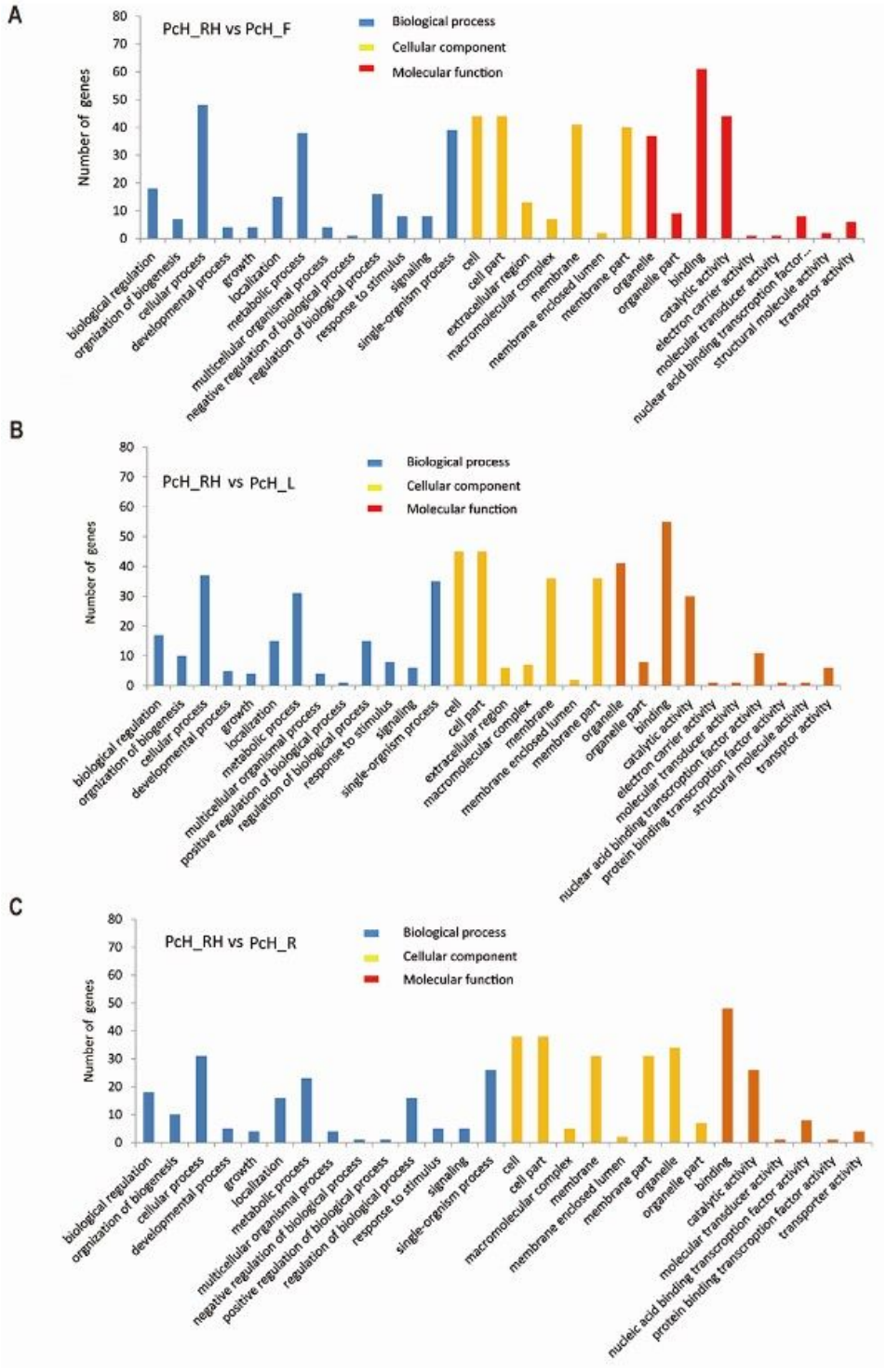

Figure 4

GO enrichment analysis of the target genes of DEMs identified in different pairwise comparisons of P. cyrtonema tissues. (a–c) Comparison of target genes in the rhizome with those in flower (a), leaf (b), and root (c). The X-axis shows the number of DEMs, and Y-axis shows the GO terms. GO terms grouped in biological process, cellular component, and molecular function are indicated in blue, brown, and red, respectively.

Figure 5

KEGG pathway enrichment analysis of target genes of the DEMs in different pairwise comparisons of P. cyrtonema tissues. (a–c) Comparison of target genes in the rhizome vs. flower (a), rhizome vs. leaf (b), and rhizome vs. root (c).

Figure 6

Abundance of DEMs and their target genes involved in carbohydrate metabolism. Abundance of DEMs (A) and target genes (B) in different tissues.

Figure 7

Expression analysis of miRNAs and their target genes in different tissues of P. cyrtonema using qRT-PCR. Data represent the mean ± standard deviation (SD) from triplicate assays

Figure 8

The 3D models and multiple sequence alignment of abfA. (a) N-terminal catalytic domain of abfA with a (β7/α8)-barrel architecture. Helices are colored in red, and strands are colored in yellow. (b) C-terminal domain of abfA (blue) with a jelly-roll topology. (c) Spatio-structural models of abfA (CL6296.Contig1) with the highly conserved binding site (W297) depicted as magenta spheres. (d) Alignment of β-AS amino acid sequences. Black indicates identical amino acids, and cyan indicates similar amino acids. The multiple sequence alignment was performed using the DNAMAN 6.0.3.99 software.

Supplementary Files

This is a list of supplementary files associated with this preprint. Click to download.

- FigureS1.tif
- FigureS4.tif
- FigureS5.tif
- FigureS3.tif
- FigureS2.tif
- SupplementaryTables.xls